Bioresource Technology Reports 27 (2024) 101875

Contents lists available at ScienceDirect

Bioresource Technology Reports

journal homepage: www.sciencedirect.com/journal/bioresource-technology-reports

Screening of pure cultures for their efficiency to convert electricity and CO_2 into methane

Benjamin Roessler [a], Sandra Off [a], Oliver Arendt [a], Johannes Gescher [b,*]

[a] Hamburg University of Applied Sciences, Competence Center for Renewable Energies, CC4E, Germany
[b] Hamburg University of Technology, Institute for Technical Microbiology, Germany

ARTICLE INFO

Keywords:
Bioelectrochemical Systems
Bioelectrochemical Power-to-Gas
EM
Microbial Electrosynthesis
In-situ Biological Methanation

ABSTRACT

The demand for defossilization and decarbonization resulting from the climate crisis and the lack of storable renewable energy has brought biomethane back into focus. Methanogenic microorganisms can be used to convert renewable energy into biomethane. In a pressurized H-cell reactor, we demonstrate the electroactivity of four different methanogenic archaea under conditions of direct and indirect electromethanogenesis. The cathodes were adjusted to a potential of −300 mV (direct electromethanogenesis) and − 700 mV (indirect electromethanogenesis) relative to a standard hydrogen electrode. At −300 mV, no significant methane formation was observed in all four cultures. At a potential of −700 mV, *Methanococcus maripaludis* achieved an average daily methane production rate of 61 mmol/m^2 per day. The highest methane concentration of 199.4 mmol/m^2 and the highest coulombic efficiency of 74.0 % were reached within 72 h by *Methanococcus maripaludis*.

1. Introduction

Anthropogenic greenhouse gas emissions have risen dramatically since the industrial revolution and are accelerating global climate change (Völler et al., 2020). The increase in global warming can be limited by defossilizing the mobility and heating sectors as well as industrial processes. One way to achieve this goal is to use renewable methane from power-to-gas technologies based on sustainable energy sources (Zhang et al., 2017). One promising power-to-gas technology is the conversion of CO_2 from a direct air capture system into storable biomethane using a bioelectrochemical system and residual electricity from renewable sources (e.g., photovoltaics and wind turbines) (Geppert et al., 2016). This biomethane has a negative greenhouse gas balance and can replace fossil natural gas (Fasihi et al., 2019; Mohan et al., 2019; Chestney, 2022). The metabolic process, electromethanogenesis (EM), was first described by Cheng et al. in 2009 (Cheng et al., 2009). They claimed that only protons and electrons are required for the conversion of CO_2 to CH_4. The protons are supplied by the medium and the electrons by the current generated by the applied voltage, see Eq. 1 (Cheng et al., 2009):

$$CO_2 + 8H^+ + 8\,e^- \rightarrow CH_4 + 2\,H_2O \quad (1)$$

The experiments of Cheng et al. were performed under conditions that allowed an abiotic hydrogen evolution reaction, starting from voltages lesser than −400 mV against a standard hydrogen electrode (SHE). The authors detected CH_4 with a small amount of hydrogen at the cathode. However, this minimally produced hydrogen could not explain the high CH_4 production in their work. Based on their experiments, they suspected a direct electrode-microbe electron transfer (Cheng et al., 2009).

Theoretically, direct electron transfer would be an advantage of this technology, as the overpotential required for the separate generation of electrolytic hydrogen would be eliminated. Less energy would therefore be required (direct EM) than with indirect EM. From an electrochemical point of view, methanogenesis or EM can take place at a standard electrode potential of $E^0 = -240$ mV vs. SHE (Ceballos-Escalera et al., 2020) without the use of hydrogen. At a standard electrode potential of $E^0 = -410$ mV vs. SHE or less, hydrogen can theoretically be generated abiotically at the electrode (Rabaey and Rozendal, 2010).

However, a literature review of relevant studies on EM revealed that most of these studies used voltages <−400 mV vs. SHE, i.e., conditions under which an abiotic hydrogen evolution reaction can at least theoretically take place (Rabaey and Rozendal, 2010). In addition, different experimental setups and different H-cell reactors were used (Table S1). Based on the experimental results found in these studies, it cannot be excluded that hydrogen is generated directly at the electrode (in-situ)

* Corresponding author.
E-mail address: johannes.gescher@tuhh.de (J. Gescher).

https://doi.org/10.1016/j.biteb.2024.101875
Received 20 March 2024; Received in revised form 28 May 2024; Accepted 3 June 2024
Available online 10 June 2024

and then converted to CH4 in a second step (Cai et al., 2020; Carrillo-Peña et al., 2022; Pelaz et al., 2023). A recent study also suggests that direct electron transfer and indirect methanogenesis could coexist (Lohner et al., 2014).

To further clarify this question and to search for electroactive microorganisms that efficiently convert excess electricity into storable CH_4, a series of experiments was conducted with four different cultures of methanogens.

Two different voltages were used for the experiments, −300 mV and − 700 mV vs. SHE. At a voltage of −300 mV, no hydrogen based on water electrolysis can be formed at the electrode under the chosen process conditions (Ceballos-Escalera et al., 2020). Still, at this potential direct electromethanogenesis could take place, in which the electric current can be converted directly into methane using carbon dioxide as electron acceptor. In contrary, a potential of −700 mV should allow for hydrogen-based methanogenesis (Ceballos-Escalera et al., 2020). A voltage of −700 mV was used because it was frequently used before for EM studies with various methanogens (Cheng et al., 2009; Siegert et al., 2015; Fu et al., 2022; Mayer et al., 2022).

Typically, such experiments have been carried out in H-cell reactors. (Park et al., 1999; Batlle-Vilanova et al., 2015; Pawar et al., 2021; Deutzmann et al., 2023; Pelaz et al., 2023). However, the construction of the H-cells is often not fully shown or described in publications (Abdollahi et al., 2022). To ensure the comparability of this study with previous publications, an H-cell reactor was constructed and used for the current-dependent cultivation of strictly anaerobic methanogens. The criteria for the reactor were a simple, robust, and reliable design, a solid connection to the power supply and a pressure resistance of up to 600 mbar. Care was also taken to ensure that the distances between the electrodes used did not vary and were as short as possible. This ensured comparability between the H-cells in the test series and kept the ohmic resistance as low as possible. The results show that the efficiency of methane production strongly depends on the strains used. Based on the experimental setup, only a methane production at −700 mV vs. SHE was observed, as methane production was not detectable at −300 mV vs. SHE.

2. Materials and methods

2.1. Strains and cultivation

Four precultures were prepared for the experiments conducted in this study: *Methanobacterium congolense* (DSM 7095), *Methanococcus maripaludis* (DSM 14266), *Methanobacterium formicicum* (DSM 2639) and an isolated subspecies of *Methanobacterium formicicum* (see the isolation strategy described in chapter 2.3).

For the isolation, a defined medium (isolation medium) according to Scherer, 1989 was used with minimal adaptations (Scherer, 1989). The macroelement solution consisted of $MgCl_2$ x 6 H_2O 1 mM, NaCl 30 mM, NH_4Cl 18.6 mM, KCl 64.1 mM and $CaCl_2$ x 6 H_2O 0.5 mM. The trace element solution used contained Graham's salt $(NaPO_3)_x$ 102 mM, $ZnCl_2$ 1 mM, $MnCl_2$ x 4 H_2O 100 µM, H_3BO_3 10 µM, $CuCl_2$ x 2 H_2O 200 µM, Na_2WO_4 x 2 H_2O 100 µM, $CoCl_2$ x 6 H_2O 300 µM, $NiCl_2$ x 6 H_2O 300 µM, Na_2SeO_3 x 5 H_2O 200 µM, Na_2MoO_4 x 2 H_2O 100 µM, and Fe-(III)-Cl_2 x 6 H_2O 2 mM. The modified Wolin's vitamin solution consisted of 8.2 µM biotin, 4.5 µM folic acid, 48.6 µM pyridoxine-HCl, 13.3 µM riboflavin, 14.8 µM thiamine-HCl, 40.6 µM niacin, 10.5 µM pantothenic acid, 0.15 µM vitamin B12, 36.5 µM 4-aminobenzoic acid and 24.2 µM lipoic acid (Wolin et al., 1964). This solution was filter sterilized.

For the isolation and pre-cultivation of the cultures, the medium contained 962 mL of the macroelement solution, 10 mL of the trace element solution, 10 mL of imidazole (2 M), and 2 mL of a resazurin solution (4 mM). After anaerobization, see section 2.2, the medium was reduced with 2 mL of cysteine solution (213 mM cysteine HCl monohydrate and 5 mM Fe-(II) citrate), 2 mL of sodium sulfide solution (250 mM Na_2S x 9 H_2O), and 1 mL of a titanium-citrate solution (200 mM tri-sodium-citrate x 2 H_2O and 83.9 mM titanium(III) chloride). As a final step, 10 mL of the sterile heat-sensitive vitamin solution was added.

The following minimal medium (electrochemical medium) was used for the bioelectrochemical experiments. The macroelement solution consisted of KCl 4.7 mM, $MgCl_2$ x 6 H_2O 19.7 mM, $MgSO_4$ x 7 H_2O 14.0 mM, NH_4Cl 4.7 mM, $CaCl_2$ x 2 H_2O 0.95 mM, K_2PO_4 0.8 mM, Fe $(NH_4)_2SO_4$ x 6 H_2O 0.01 mM, NaCl 308.0 mM, MOPS buffer 99.9 mM, $NaHCO_3$ 59.5 mM. The trace element solution contained Titriplex I 7.85 µM, $MgSO_4$ x 7 H_2O 12.17 µM, $MnSO_4$ x H_2O 2.96 µM, NaCl 17.11 µM, $FeSO_4$ x 7 H_2O 0.36 µM, $CoSO_4$ x 7 H_2O 0.64 µM, $ZnSO_4$ x 7 H_2O 0.63 µM, $CuSO_4$ x 5 H_2O 0.04 µM, $AlK(SO_4)$ x 12 H_2O 0.04 µM, H_3BO_3 0.16 µM, Na_2MoO_4 x H_2O 0.04 µM, $NiCl_2$ x H_2O 0.23 µM, Na_2SeO_3 x 5 H_2O 1.14 µM, and Na_2WO_4 x H_2O 1.66 µM. Before anaerobization and sterilization, 10 mL of the trace element solution was added to 980 mL of the macroelement solution. After sterilization, 10 mL of the vitamin solution described above was added. The media were reduced by adding 4 mL of the cysteine solution and 100 mL of the titanium-citrate solution.

2.2. Anaerobization procedure

The experiments were carried out under strictly anoxic conditions. The required conditions were achieved as follows: The medium in the serum bottles was stirred and a vacuum was applied to remove the oxygen dissolved in the liquid. Nitrogen gas (purity 5.0) was then introduced into the headspace at a pressure of 1 bar. This process was repeated three times. The anaerobic serum bottles were flushed with H_2:CO_2 gas (80,20, purities: H_2 5.0 and CO_2 3.5) via a sterile cannula. The gas was supplied at 2 bar for 5 s. The anaerobization of the H-cells differed from that in the serum bottles. Here, the medium was flushed with 0.5 bar nitrogen for 15 min to replace the oxygen. In the electrochemical experiments, N_2:CO_2 (80,20, purities: N_2 4.5 and CO_2 5.0) was used. For this purpose, a cannula was inserted via a reactor opening and the gas was used to purge the headspace above the medium with a constant flow for 20 s, while a second cannula was inserted via a septum on the lid as a gas outlet to avoid the formation of overpressure. At the end, the cannula was removed from the septum and the reactor was pressurized with the feed gas for another 20 s.

2.3. Isolation procedure

In this study, an isolation strategy was carried out to separate methanogens from the fermentation sludge of a biogas plant sample (Eschede, northern Germany, main feed: horse manure). These methanogens were isolated under electrochemical conditions by an applied voltage of 0.5 V. This isolation was performed to find a methanogen that could better interact with a cathode compared to already used methanogens for electro-biotechnological processes. A similar vessel design was used for the isolation as in Call et al. 2011 (Call and Logan, 2011). The isolation of an electroactive methanogen was carried out by diluting the fermentation sludge of a biogas plant in a ratio of 1:10 with the isolation medium using various antibiotics (ampicillin, vancomycin, streptomycin, bacitracin, kanamycin, nalidixic acid). After one week, the cathode was transferred to a new vessel. This step was repeated three times under a CO_2 atmosphere (purity 99.7 %) with a pressure of 0.5 bar and an applied voltage of 0.5 V using a DC laboratory power supply. After the third transfer, the atmosphere was replaced with H_2:CO_2 (80:20, purities: H_2 5.0 and CO_2 3.5) to ensure optimal growth of the isolated methanogens. This step was repeated twice. During this procedure, the growth of the cells was observed with a fluorescence microscope at a wavelength of 420 nm.

2.4. Microbial and taxonomic characterization of the isolate

The taxonomic evaluation of the isolate was performed by 16S rRNA amplicon sequencing following Maus et al. (Maus et al., 2017). For a more detailed taxonomic description of the isolate, genes of methyl-

coenzyme M reductase (*mcrA* genes) were analyzed with the following primers: ME1f (5'-GCM ATG CAR ATH GGW ATG TC-3′) and ME2r (5'-TCA TKG CRT AGT TDG GRT AGT-3′) (Nettmann et al., 2008). The PCR product was amplified with the following program: Initial denaturation at 94 °C for 4 min, 30 cycles of denaturation at 94 °C for 40 s, annealing at 50 °C for 45 s and elongation at 72 °C for 90 s. The final extension lasted 6 min at 72 °C (Battumur et al., 2016). The amplified PCR product was sequenced using Sanger sequencing (LGC; Berlin). In addition to the taxonomic description, the pH and temperature optima were also investigated using growth experiments. The pH range was determined with 100 mM imidazole buffer (6.0 to 7.5) and 100 mM HEPES (7.5 to 8.5) in steps of 0.5 pH units. The optimum temperature was determined in a range from 20 °C to 55 °C using the following temperatures: 20, 37, 39, 41, 45, 50, 55 °C.

2.5. Construction of the H-cell

Fig. 1 shows all parts for the construction of the H-cell reactor and the fully assembled reactor. All components can be autoclaved, except for the Ag/AgCl wire of the reference electrode (part 9), which must be added afterwards. The lid, part 5, was made of polyether ether ketone (PEEK). The lid contained three screw holes with a diameter of 6 mm for the electrodes and the gas extraction. The gas sampling opening was sealed with a septum made of butyl rubber. The electrode holder, part 8, also had a diameter of 6 mm and was fastened with a hollow screw and an O-ring. The connection to the potentiostat was ensured by a double-diameter hole for the 2 mm plug on the top of the electrode holder.

The glass body of the reference electrode (part 9, diameter 6 mm) was inserted into the electrode opening of the lid. After the sterilization process, the Ag/AgCl wire was inserted into the glass body, which was filled with a 3 mM KCl solution. The tightness of the electrodes in the ports was ensured with a sealing ring and a hollow screw (part 7). The fully assembled lid was screwed onto the glass body (part 1) with a flat sealing ring (part 6) and a screw cap (part 4). The pre-treated Nafion™ 117 membrane (QuinTech, not shown) was inserted between the two silicone sealing rings (part 2). The three compartments were connected to the two glass bodies with a QF clamping chain (part 3). The pre-treatment of the Nafion membrane served to improve the proton conductivity between the cathode and anode chambers (Scott and Yu, 2015; Jiang et al., 2016). For this purpose, the membrane was protonated by immersing it in a 3 % H_2O_2 solution for one hour. Subsequently, the membrane was immersed for two hours in dd. H_2O. Finally, the membrane was soaked in 0.5 mM H_2SO_4 for one hour and then rinsed with dd. H_2O and stored (Jiang et al., 2016; Kuwertz et al., 2016; Baek et al., 2017).

The structure of the H-cell described here was designed in such a way that a specially constructed lid ensures a constant distance between the working and counter electrodes (85 mm) and between the reference electrode and the working electrode (15 mm). This fixed distance enables good comparability between the different test series and within the optimum range for chronoamperometric measurements in H-cells, as described by Song et al. (Song et al., 2019).

2.6. Analytical methods

The quantitative microscopic fingerprinting (QMF) method was used to determine cell growth over time using a Leica DM6000B microscope. This method was previously described by Kim et al. (Kim, 2014). In addition, pH and electrical conductivity were measured in triplicate.

2.7. Gas analysis

Gas samples were taken from the headspace of the glassware and analyzed using the Agilent 7890B series gas chromatograph. For analysis values >100 ppm two thermal conductivity detectors were used, for gas components <100 ppm a methanizer and a flame ionization detector were used. The gas samples were taken with gas-tight 5 mL syringes.

2.8. Electrochemical experiments

2.8.1. Chronoamperometry

Electrochemical experiments were performed with a potentiostat from Biologic (France, Claix) and an Ag/AgCl electrode as reference. To determine the electrical activity of methanogens, chronoamperometric measurements were performed at two different cathode potentials: −300 mV and − 700 mV (against standard hydrogen electrode, SHE). Electron consumption was recorded every 60 s. The coulombic efficiency (CE) was calculated as follows:

$$CE = \frac{n_{measured}}{n_{calculated}}; n_{calculated} = \frac{\int_0^t I\,dt}{z\,x\,F} \quad (2)$$

where $n_{measured}$ is the measured amount of methane from the gas chromatographic analysis and $n_{calculated}$ is the theoretical amount of methane

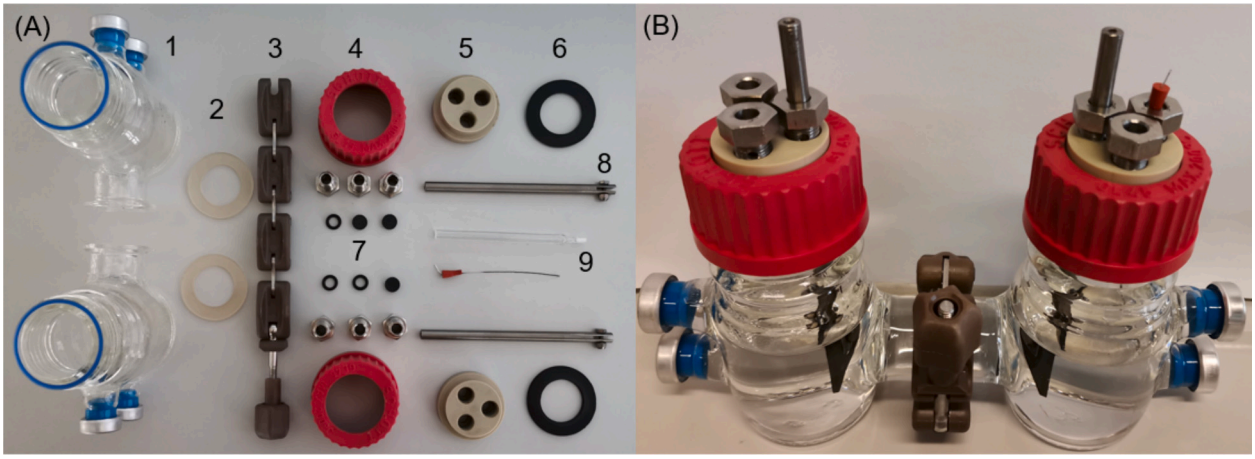

Fig. 1. (A) Components of an H-cell reactor (except the carbon electrodes) and (B) fully constructed H-cell reactor. 1: 100 mL Glass bodies (Schott flask) with a 20 mm diameter glass bridge connector, blue chlorobutyl rubber stopper and aluminum seals; 2: Silicon flat sealing rings, DN25, natural-colored: transparent; 3: QF clamp chain with a diameter of DN25; 4: Screw caps with hole; 5: PEEK lid with three M10 holes; 6: Flat sealing rings, GL14; 7: Hollow screws, septa and O-rings, with a diameter of 6 mm made of stainless steel and butyl rubber respectively; 8: Electrode holder with titanium (grade 2) screws and nuts; 9: Glass body for reference electrode with magnesium frit and silver chloride coated silver wire and silicone stopper. (For interpretation of the references to colour in this figure legend, the reader is referred to the web version of this article.)

produced. The latter is determined by the measured current density $\int_0^t I\,dt$ over a certain time interval. Additional quantities are the number of electrons needed to produce methane from carbon dioxide z (8 electrons for methane) and Faraday's constant F with 9.64853×10^4 A s/mol.

2.8.2. Bio-electrochemical set-up

The bioelectrochemical experiments were carried out in the H-cell reactors and all used voltages refer to a standard hydrogen electrode. For each type of methanogen, two reference reactors and three reactors incubated with microorganisms were used to collect sufficient data. The microorganisms were inoculated in the cathodic chamber with an initial cell density of 1×10^7 cells per mL and incubated at 41 °C. The experiment started with a voltage of −300 mV for 168 h, with a sample interval every 24 h (four times) and once after 72 h. After cultivation at −300 mV, the voltage in the reactor was set to −700 mV for a further incubation of 168 h, with the same sample interval as at −300 mV.

The electrochemical medium was used as anolyte and catholyte. The anodic and cathodic electrodes were set up in the same way. The graphite electrodes (POCO, EDM-3) were firmly attached to the bottom of the electrode holders (see Fig. 1, part 8) with a titanium screw and a fixing nut. The graphite electrodes had a surface area of 10 cm^2. The total surface area of each electrode including the immersed rod was 13.6 cm^2. To investigate direct EM, a cathode potential of −300 mV was applied while indirect EM was evaluated using a cathode potential of −700 mV. Gas composition and pressure were measured daily using a gas-tight syringe. The pH value, cell count, and electrical conductivity were measured weekly. A liquid sample of 1 mL was taken from the lower port using a cannula. All bioelectrochemical experiments were carried out in triplicate, except for culture EE, which was carried out in duplicate due to a reactor malfunction.

2.9. Scanning electron microscope

In addition to observing the microbial and chemical parameters, the surfaces of the electrodes used in the experiments were analyzed via scanning electron microscope. For this precise microscopic examination, the electrodes were incubated for 24 h in a 3 % glutaraldehyde solution. The electrodes were then washed three times at 15-min intervals in phosphate-buffered saline, followed by a series of 50, 70 and 90 % (vol.) ethanol concentrations for 20 min each. Finally, the electrodes were washed three times in 100 % ethanol for 20 min (Zakaria et al., 2018). The fixed and washed electrodes were sputtered with gold for higher resolution. Images of the electrodes were captured using a scanning electron microscope (FEG-REM LEO 1530, Zeiss, Germany) with an Everhart-Thornley detector. The experiments were carried out at the Department of Electron Microscopy (BeEM) at the Hamburg University of Technology (TUHH).

3. Results

3.1. Isolation of a methanogen under bio-electrosynthesis conditions

Various methanogens are used in EM research and their electroactivity was investigated (Cheng et al., 2009; Mayer et al., 2019; Rowe et al., 2019). Here, a methanogen was isolated from a biogas plant fed with liquid manure and maize. The aim was to find out whether isolation under the desired process conditions would lead to an organism with advanced capabilities in terms of cathode-driven methane production compared to previously used model organisms. The Sanger sequencing revealed 99.5 % similarity to the archaeon *Methanobacterium formicicum*. The result of the 16S rRNA amplicon sequencing analysis confirmed that the isolate was a pure culture which was further referred to as culture EE. The raw amplicon data have been deposited with ENA/GenBank/DDJB under the bioproject ID PRJEB65119. The *mcrA* genes were analyzed for a more detailed taxonomic description of the isolate. The results of the Sanger sequencing showed that at least two different *mcrA* genes are involved in the synthesis of the methyl-coenzyme M reductase. In the following results, the isolate is referred to as culture EE. The optimal pH range of culture EE was determined to be between 6.5 and 7.5 while the optimal temperature is 41 °C (data not shown).

3.2. Comparative bioelectrochemical experiments

The isolated strain EE was compared with the strains *Methanobacterium formicicum*, *Methanococcus maripaludis* and *Methanobacterium congolense* regarding cathodic methane production. The pH values and the electrical conductivity of the bioelectrochemical setups were analyzed once a week during the experiments. The pH value in the cathode chamber was stable at 7.2 and the electrical conductivity increased slightly from 17 mS/cm^{-1} to 22 mS/cm^{-1}. The measured pressure remained stable at 0.55 mbar throughout the experiments and showed only slight fluctuations which were probably due to minimal gas losses. The gas phase in the reactors was analyzed every 24 h and thereafter replaced by sparging with N_2:CO_2 (80:20). After four days the experiment was carried out for an additional 72 h interval before the gas phase was analyzed.

In abiotic control experiments, no hydrogen production was observed at a voltage of −300 mV. At a voltage of −700 mV, hydrogen evolution took place with an average production of 344 ± 68 $mmol/m^2$ per day. As expected, 1015 ± 176 $mmol/m^2$ hydrogen was produced within the 72 h time interval (Fig. 2).

In the biotic experiments operated at a cathodic voltage of −300 mV aiming to reveal direct cathode-microbe electron transfer, CH_4 was not detectable regardless of the organism used. H_2 could only be detected in some experiments at the very beginning, probably due to the inoculation with precultures cultivated under an H_2:CO_2 (80:20) atmosphere. If a detectable CH_4 concentration was present at the beginning, it dropped asymptotically to zero in all experiments (Fig. 3). (See Figs. 2 and 3.)

After switching to −700 mV, an increase in hydrogen and methane concentration was observed in all cultures. The culture of *Mc. maripaludis* consumed almost all available electrochemically produced hydrogen within the four 24 h intervals. This relates on average to 61 mmol methane per m^2 of cathode surface and day. Within the 72 h time interval, a maximum methane concentration of 199.4 $mmol/m^2$ was measured for *Mc. maripaludis* (Fig. 3). Compared to this culture EE produced within the same time interval 136.7 $mmol/m^2$. Still, the cultures of *Mb. formicicum* and *Mb. congolense* were not able to consume all cathodically produced hydrogen and consequently produced significantly less methane (Fig. 3).

Reductive current development was also measured during the experiments. No significant change in current density could be observed over time when the electrodes were poised to −300 mV (Fig. 4). This changed during the second part of the experiments when the cathode potential was decreased to −700 mV. The chronoamperometric measurements showed that the current densities decreased for all methanogens tested over the course of 24 h (Fig. 4). The smallest decrease in current density at the end of the fourth 24-h cycle (IV. 24 h) was measured for *Mb. congolense* (−462 mA per m^2 electrode area). The largest difference was observed for *Mc. maripaludis*. Here current density decreased to −991 mA/m^2. Nevertheless, a direct correlation between methane productivity and increase of reductive current was not detectable for the cultures. Culture EE and *Mb. formicicum* had a significantly different methane production but the current density development was rather similar. While hydrogen depletion at the cathode by the methanogens will most likely play a role for the development of the reductive current, the results indicate that other factors might also play a role.

The coulombic efficiency (CE) describes the conversion of the electrical current into the target product, in this case methane (Fig. 5). In each 24-h step and in the long-term step, the CE increased constantly for EE and *Mc. maripaludis* and reached for *Mc. maripaludis* with 74.0 % the

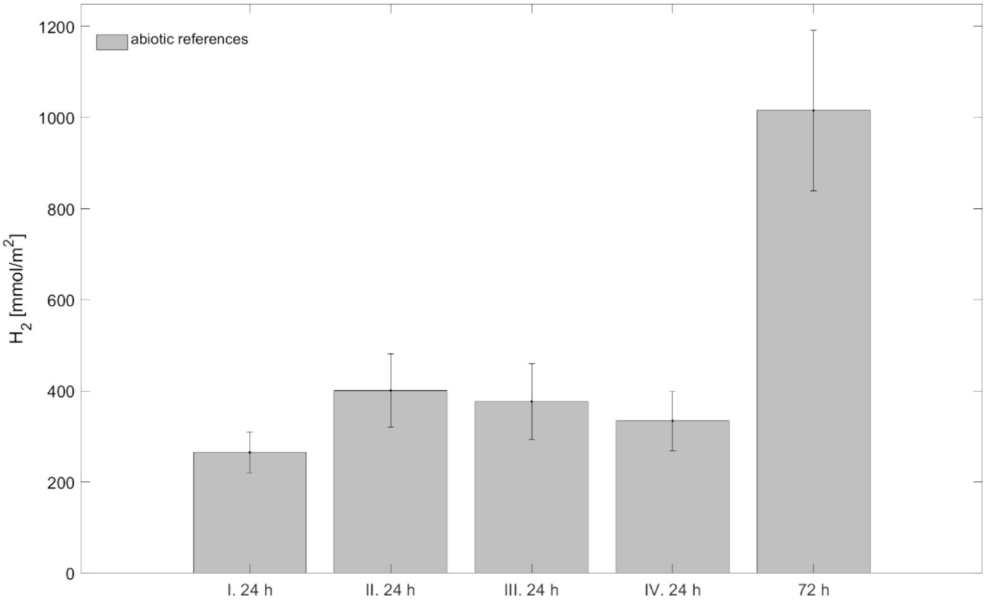

Fig. 2. Hydrogen production under abiotic conditions using cathodes poised to −700 mV. The amounts of hydrogen shown here are in mmol per m^2 of cathode surface for four consecutive measurement intervals of 24 h and one long-term experiment of 72 h.

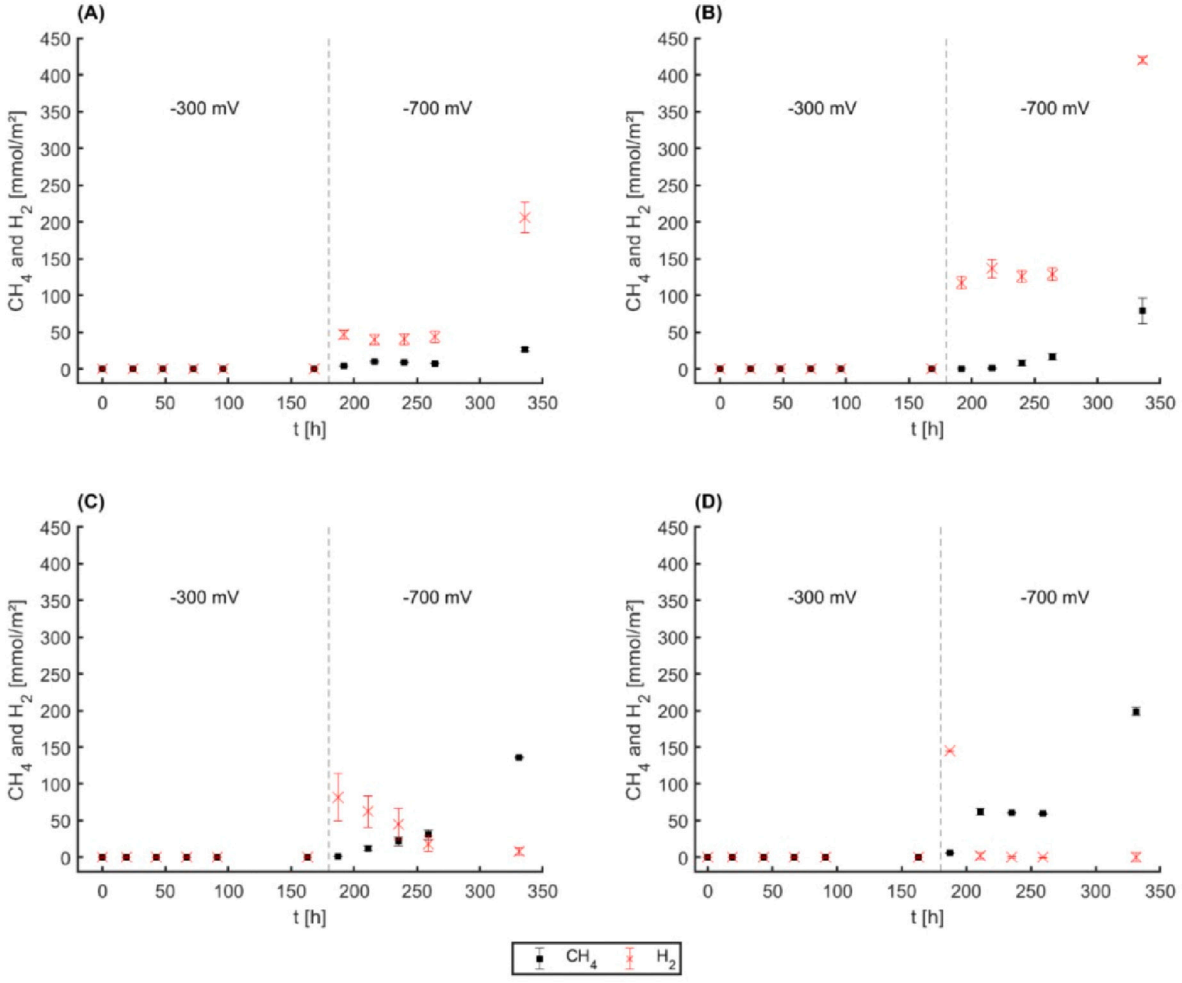

Fig. 3. Methane and hydrogen production referred to the cathodes surfaces at a voltage of −300 mV and − 700 mV. (A) *Methanobacterium congolense*, (B) *Methanobacterium formicicum*, (C) culture EE, (D) *Methanococcus maripaludis*.

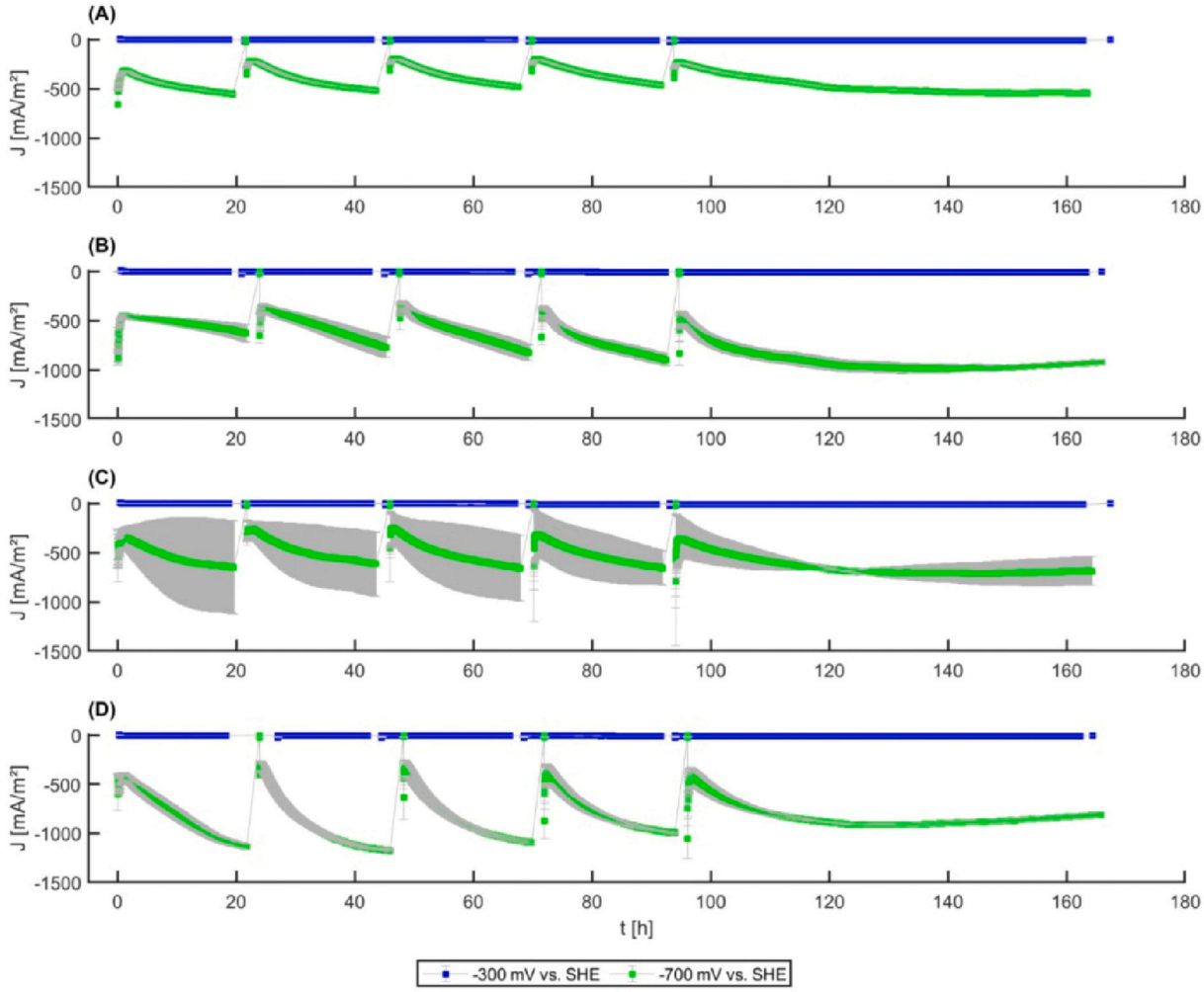

Fig. 2. Chronoamperometric measurements at −300 mV (blue) and − 700 mV (green). The mean deviation was calculated from at least two identical sets (light gray). (A) *Methanobacterium congolense*, (B) *Methanobacterium formicicum*, (C) culture EE, and (D) *Methanococcus maripaludis*. (For interpretation of the references to colour in this figure legend, the reader is referred to the web version of this article.)

highest value. However, *Mb. congolense* and *Mb. formicicum* only reached a maximum CE of 20.4 % and 26.3 %, respectively (Table 1). As depicted in Fig. 5, CE development leveled for all organisms towards the end of the experiment at the latest, which suggests that the time under these conditions was sufficient to adapt to electrode dependent growths. Although it cannot be exclude that adaptations of *M. congolense* and *Mb. formicicum* to process conditions could increase CE further, both strains remain behind at least within the time frame of the conducted experiments.

3.3. Development of biomass during the experiments

The QMF method was used to quantify the living planktonic cells. At the beginning of the experiments, all cultures were inoculated with a cell density of approximately 1×10^7 cells/mL. During cultivation at a voltage of −300 mV, the cell number of *Mb. congolense* decreased 2-fold and the cell number of *Mb. formicicum* 1.5-fold. For *Mc. maripaludis* the cell count lowered 3.5-fold from the beginning to the end of the first part of the experiment at a voltage of −300 mV. However, the EE culture is the only culture that shows a slight but statistically not significant increase in cell number by 1.2-fold.

The electrode potential was then switched to −700 mV without a reinoculation. During this second part of the experiment, an increase in cell density of 1.2-fold and 2.3-fold was measured for *Mb. congolense* and *Mb. formicicum*. The cell number for the culture EE increased 1.4-fold and for the culture *Mc. maripaludis* >10-fold compared to the cell numbers at the end of −300 mV step (Table 2).

Besides quantifying planktonic cells, we also analyzed potential biofilm formation on the electrodes at the end of the experiments conducted at −700 mV. The electrodes were fixed with 3 % glutaraldehyde to analyze growth using scanning electron microscopy. Fig. 6 (A) and (B) show the growth of *Mb. congolense* and *Mb. formicicum* on the respective electrodes. In both cases, only slight growth can be seen. Although *Mb. formicicum* grew comparably well in the planktonic phase, it was apparently low biofilm formation that led to the low methane production. In contrast, Fig. 6 (C) shows almost complete coverage of the graphite electrode with a biofilm of the EE culture. Fig. 6 (D) shows *Mc. maripaludis*. Here, both groups and individual cells of the coccoid organism cover the cathode surface almost completely.

4. Discussion

Can electromethanogenic productivity and coulombic efficiency be correlated with specific answers of methanogens to process conditions? To answer this question, four different pure cultures of methanogens were tested in this study. Three available pure methanogens from the DSMZ and one methanogen isolated under electroactive conditions (culture EE) were examined. We hypothesized that the isolate might

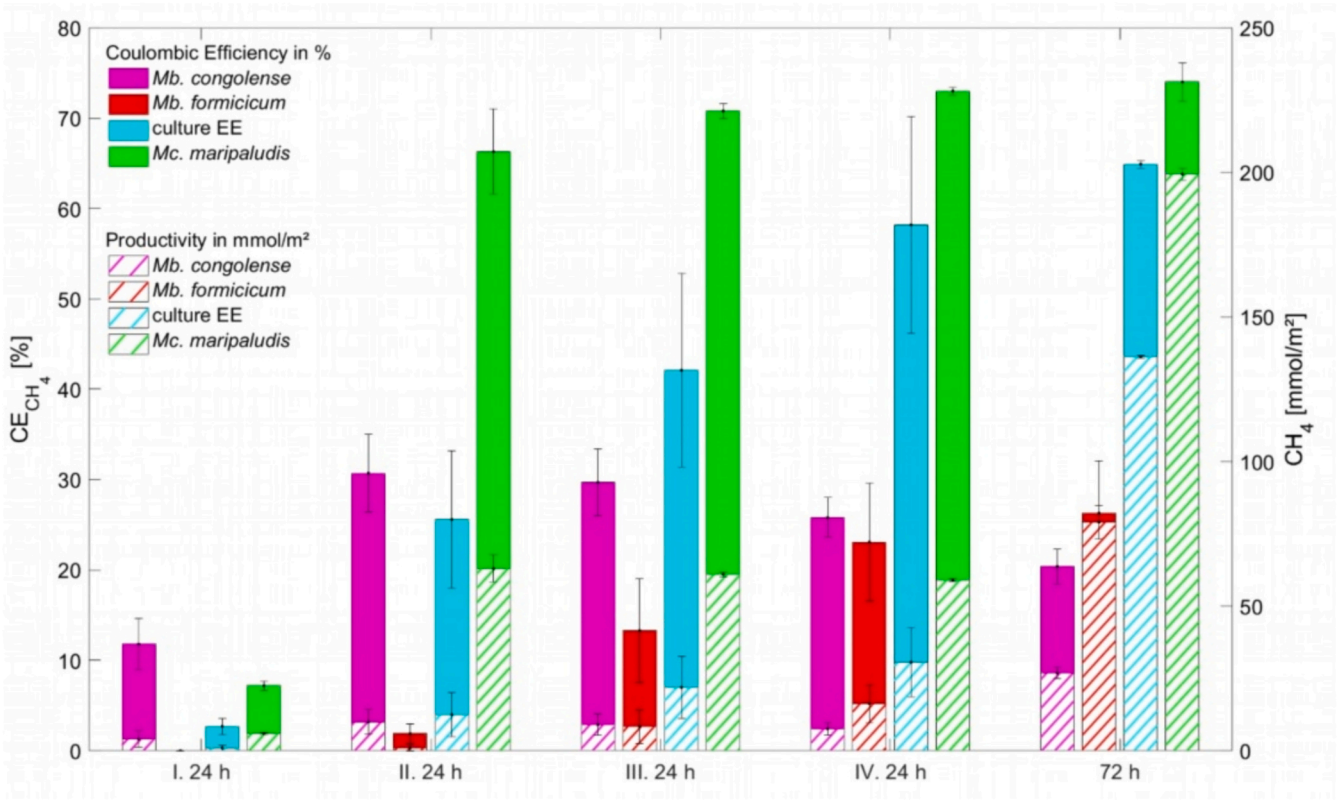

Fig. 3. Coulombic efficiency of all cultures combined with the effective methane production within four subsequent measurement intervals of 24 h and one long term experiment over 72 h at a voltage of −700 mV.

reveal best catalyst characteristics as it was isolated under similar conditions compared to chosen process regime.

The culture EE, obtained from a biogas plant fed with horse manure, showed a genetic similarity of 99.5 % with *Methanobacterium formicicum* based on sequencing of the 16S rRNA amplicon. The culture EE also has two different genes for methyl-coenzyme M reductase which is unique to *Methanobacterium formicicum* strains (Hallam et al., 2004; Xavier et al., 2020; Schorn et al., 2022). Similarly, the pH and temperature optima are also consistent with the results obtained for other *Methanobacterium formicicum* strains, pH 7 and 37–45 °C (Battumur et al., 2016; Burdukiewicz et al., 2018).

The activity of methanogens in direct EM was tested at a voltage of −300 mV. This potential should be suitable for direct electromethanogenesis, occurring theoretically at potentials below −240 mV vs. SHE (Song et al., 2019) but too low for direct abiotic hydrogen evolution. During the experiments at −300 mV, the residual concentrations of hydrogen and methane resulting from the inoculation dropped to zero within a few hours. The formation of new methane or hydrogen due to cathodic activity was not detectable for any of the four methanogens. This suggests that no measurable direct EM took place. This result is also confirmed by the mean current, in which no significant differences in potential were detectable when biotic and abiotic experiments were compared. This result is corroborated by similar studies conducted in other research groups (Aulenta et al., 2011; Blanchet et al., 2015). In both cases, no measurable methanogenic activity was observed at a voltage of −300 mV.

The second voltage was set to −700 mV v. SHE to investigate indirect EM. Of note, this voltage has also been used in a number of previous studies on electromethanogenesis (Cheng et al., 2009; Lohner et al., 2014; Enzmann and Holtmann, 2019). The results showed that, in contrast to the −300 mV-experiments, electrochemical production of hydrogen and corresponding production of methane took place (Cai et al., 2020). A daily methane production of 61 mmol per m^2 of cathode surface was achieved for *Mc. maripaludis* and 21.7 mmol/(m^2 d) for the culture EE. Other publications achieved production rates of 10.8 mmol/(m^2 d) and 11.7 mmol/(m^2 d) with *Mc. maripaludis* (Enzmann and Holtmann, 2019; Mayer et al., 2022). In addition, an increase in the cell number was measured in all experiments. However, direct uptake of electrons by the methanogens could not be ruled out (Lohner et al., 2014). Still, due to the high conversion rate of the hydrogen produced, the possible pathway of direct EM can only play a minor role, at least in the organisms used here. Interestingly, the current density did not develop uniformly for the four tested cultures but seemed to be a specific signature of the strains.

To find the most suitable of the four methanogens for EM, the efficiencies were compared with each other. Interestingly, the addition of the individual strains after changing the potential to −700 mV against (SHE) led to different developments in the current density. This did not correlate with the amount of methane that was produced by the strains. Hence, it must be assumed that the interaction of the biological material with the electrode surface initiated an electrode activation. This activation or reduction of the overpotential was not only due to hydrogen depletion based on the metabolism of the microorganisms. Along these lines, several studies conducted with *Mc. maripaludis* indicated the function of released enzymes for the electroenzymatic production of small molecules like formate or hydrogen that could then be used by the whole cell biocatalysts. These enzymes could lower the overpotential and lead to higher reductive current densities at the applied potentials (Lohner et al., 2014; Deutzmann et al., 2015; Lienemann et al., 2018). It is worth to mention, that the addition of *Mc. maripaludis* led to highest current densities measured in this study. Other studies suggested that not even intact enzymes might be necessary to lower the overpotential. However, the biomass could also lead to an electrode activation by an increase of metals at the electrode surface, which could have been part of catalytic centers of metalloenzymes (Yates et al., 2014). The amount and nature of different factors released by the individual organisms

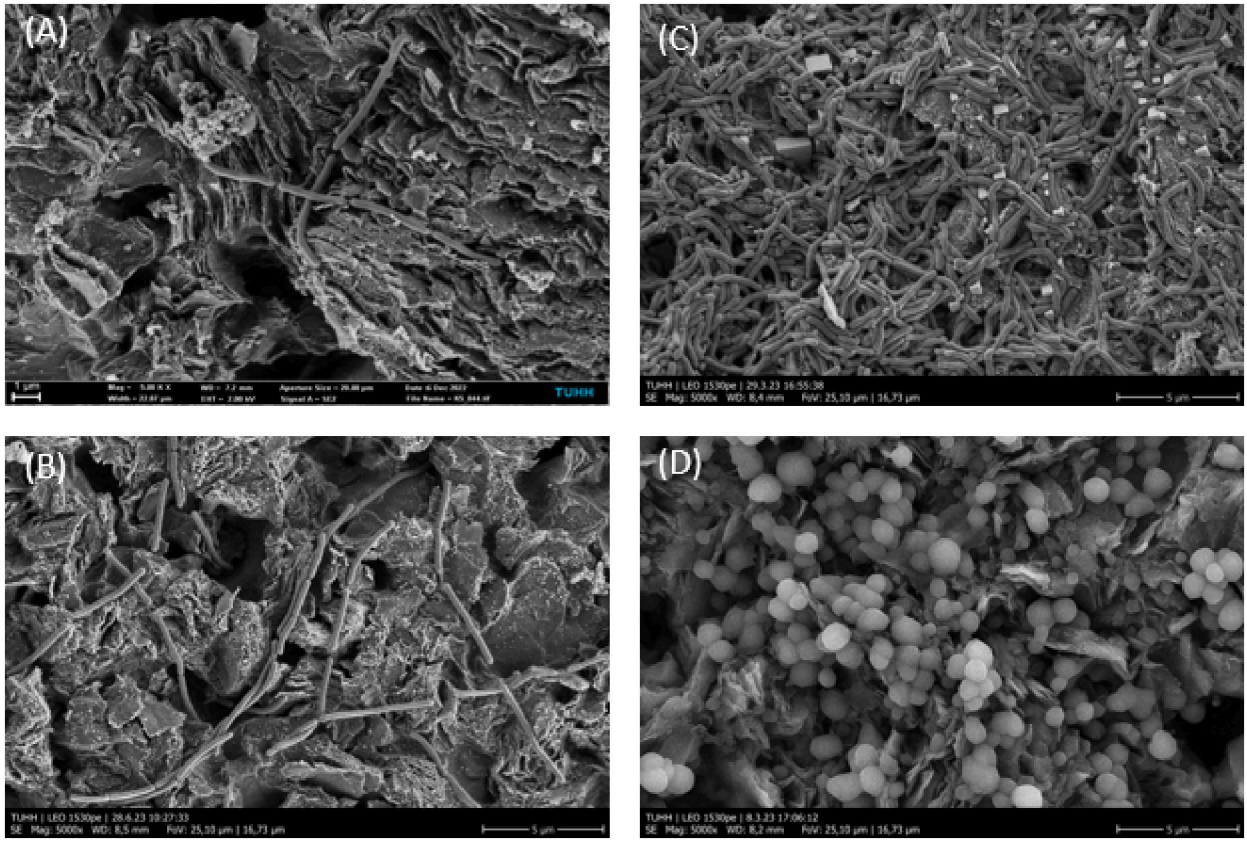

Fig. 4. SEM pictures of (A) *Methanobacterium congolense,* (B) *Methanobacterium formicicum,* (C) culture EE, and (D) *Methanococcus maripaludis* after the cultivation at −700 mV. *Mc. maripaludis* was coated with a gold layer to increase the conductivity for a higher resolution. (For interpretation of the references to colour in this figure legend, the reader is referred to the web version of this article.)

Table 1
Key electrical parameters of the EM, coulombic efficiency, and methane concentration. The data represent the last long-term experiment over 72 h at −700 mV vs. SHE. Each value is the mean value of three replicates with mean deviation as error. The methane production referred to cathodes surface.

Organism	mA h	CE $_{CH4}$%	CH_4 mmol m^{-2}
Mb.[1] *congolense*	29.5 ± 3.6	20.4 ± 1.9	26.9 ± 2.4
Mb.[1] *formicicum*	67.2 ± 2.8	26.3 ± 5.8	78.9 ± 17.5
Culture EE	46.9 ± 0.9	64.9 ± 0.4	136.3 ± 0.7
Mc.[2] *maripaludis*	60.3 ± 0.2	74.0 ± 2.1	199.4 ± 5.6

[1] *Methanobacterium,* [2]*Methanococcus.*

together with the metabolic hydrogen uptake will likely lead to the observed differences in current density and it will be interesting to follow this in future studies. In this study, a coulombic efficiency of <12 % was achieved in all experimental approaches within the first 24 h after application of a voltage of −700 mV. On the second day of the experiments (II. 24 h), the CE increased to 66.3 % for *Mc. maripaludis* and to 25.6 % for the culture EE. After the 72 h periods CE of 64.9 % was achieved for the culture EE and 74.0 % for *Mc. maripaludis*. Comparable results were also shown in other publications (Mayer et al., 2019, 2022; Song et al., 2019). The pure cultures of *Mb. formicicum* and *Mb. congolense* used showed a CE of only 26.3 % and 20.4 % respectively. In correlation with the CE, the methane production rate at −700 mV of both cultures increased within the 24-h measurements from 1 mmol/(m^2 d) to 31 mmol/(m^2 d) for EE and from 6 mmol/(m^2 d) to 61 mmol/(m^2 d) for *Mc. maripaludis*. Within the long period of 72 h a methane production rate of 199 mmol/m^2 was achieved by *Mc. maripaludis*, and so a calculated daily production rate of 66 mmol/(m^2 d).

The CE of *Mc. maripaludis* and culture EE appear to correlate with the ability to form biofilms on electrodes. After the test periods of 168 h at a voltage of −700 mV, the optical evaluations of the scanning electron microscope images showed that *Mc. maripaludis* and EE had formed a significantly thicker biofilm on the cathode compared to the other two methanogens examined. Interestingly, the electromethanogenic activity of the *Mc. maripaludis* type strain was higher compared to the strain that was isolated under electromethanogenic conditions. Following the dogma in microbiology: *everything is everywhere but the environment selects* (Baas Becking, 1934). It can be asked why a strain was isolated that is apparently not characterized by highest turnover rates, which should be accompanied with highest biomass production rates. One reason for

Table 2
Cell count of the investigated methanogens at −300 mV and − 700 mV.

Organism	Start concentration as Cells per mL	Cells per mL at −300 mV	Cells per mL at −700 mV
Mb.[1] *congolense*	$6.1 \times 10^6 \pm 1.7 \times 10^6$	$2.8 \times 10^6 \pm 7.6 \times 10^5$	$3.5 \times 10^6 \pm 9.3 \times 10^5$
Mb.[1] *formicicum*	$1.4 \times 10^7 \pm 8.8 \times 10^5$	$8.9 \times 10^6 \pm 6.9 \times 10^4$	$2.1 \times 10^7 \pm 2.9 \times 10^6$
Culture EE	$1.3 \times 10^7 \pm 1.7 \times 10^6$	$1.6 \times 10^7 \pm 3.8 \times 10^6$	$2.3 \times 10^7 \pm 5.0 \times 10^6$
Mc.[2] *maripaludis*	$1.5 \times 10^7 \pm 2.4 \times 10^6$	$4.1 \times 10^6 \pm 1.3 \times 10^6$	$4.4 \times 10^7 \pm 1.5 \times 10^6$

[1] *Methanobacterium,* [2]*Methanococcus.*

this could be that the current-dependent isolation process was not conducted long enough. As a result, the used strain could not form a sufficient biomass to achieve similar methane production rates as *Mc. maripaludis*. Another reason could be that the isolate might not be the methanogen with highest turnover rates but with biofilm formation characteristics that allow fast electrode coverage with a strong biofilm matrix. Notably previous research revealed that the formation of the biofilm matrix can indeed prevent the invasion of other species into a clonal biofilm culture (Dunsing et al., 2019; Bond et al., 2021).

Nevertheless, it seems that hydrogen uptake during diffusion of this gas through a biofilm matrix aids in process efficiency compared to planktonic cultures in which hydrogen losses might be more likely. Consequently, future reactor development for large scale electro-methanogenesis should specifically focus on materials and strains that support biofilm formation as well as reactor configurations in which biofilm development can be steered at least to some extent.

Supplementary data to this article can be found online at https://doi.org/10.1016/j.biteb.2024.101875.

Funding

This work was supported by the German Federal Ministry of Education and Research (BMBF), FKZ: 13FH1E01IA and 13FH1E05IA.

CRediT authorship contribution statement

Benjamin Roessler: Writing – original draft, Methodology, Investigation, Data curation, Conceptualization. **Sandra Off:** Writing – review & editing, Supervision, Methodology, Conceptualization. **Oliver Arendt:** Writing – review & editing, Methodology, Conceptualization. **Johannes Gescher:** Writing – review & editing, Supervision.

Declaration of competing interest

The authors declare no conflict of interest.

Data availability

Data will be made available on request.

Acknowledgments

A special thanks goes to Hans-Peter Bertelsen for the construction and manufacture of the individual parts of the H-cells. Also, thanks are due to Yong Sung Kim for the basic idea of this project.

References

Abdollahi, M., Al Sbei, S., Rosenbaum, M.A., Harnisch, F., 2022. The oxygen dilemma: the challenge of the anode reaction for microbial electrosynthesis from CO2. Front. Microbiol. 13.

Aulenta, F., Tocca, L., Verdini, R., Reale, P., Majone, M., 2011. Dechlorination of trichloroethene in a continuous-flow bioelectrochemical reactor: effect of cathode potential on rate, selectivity, and electron transfer mechanisms. Environ. Sci. Technol. 45, 8444–8451.

Baas Becking, L.G.M., 1934. Geobiologie of inleiding tot de milieukunde (in Dutch). In: Van Stockum, W.P. (Ed.), Vol. 1. Den Haag, Netherlands, 263 p.

Baek, G., Kim, J., Lee, S., Lee, C., 2017. Development of biocathode during repeated cycles of bioelectrochemical conversion of carbon dioxide to methane. Bioresour. Technol. 241, 1201–1207.

Batlle-Vilanova, P., Puig, S., Gonzalez-Olmos, R., Vilajeliu-Pons, A., Balaguer, M.D., Colprim, J., 2015. Deciphering the electron transfer mechanisms for biogas upgrading to biomethane within a mixed culture biocathode. RSC Adv. 5, 52243–52251.

Battumur, U., Yoon, Y.-M., Kim, C.-H., 2016. Isolation and Characterization of a New Methanobacterium formicicum KOR-1 from an Anaerobic Digester using Pig Slurry. Asian Australas. J. Anim. Sci. 29, 586–593.

Blanchet, E., Duquenne, F., Rafrafi, Y., Etcheverry, L., Erable, B., Bergel, A., 2015. Importance of the hydrogen route in up-scaling electrosynthesis for microbial CO 2 reduction. Energ. Environ. Sci. 8, 3731–3744.

Bond, M.C., Vidakovic, L., Singh, P.K., Drescher, K., Nadell, C.D., 2021. Matrix-trapped viruses can prevent invasion of bacterial biofilms by colonizing cells. eLife 10.

Burdukiewicz, M., Gagat, P., Jabłoński, S., Chilimoniuk, J., Gaworski, M., Mackiewicz, P., Marcin, Ł., 2018. PhyMet2: a database and toolkit for phylogenetic and metabolic analyses of methanogens. Environ. Microbiol. Rep. 10, 378–382.

Cai, W., Liu, W., Wang, B., Yao, H., Guadie, A., Wang, A., 2020. Semiquantitative Detection of Hydrogen-Associated or Hydrogen-Free Electron Transfer within Methanogenic Biofilm of Microbial Electrosynthesis. Appl. Environ. Microbiol. 86 (17), 1–11.

Call, D.F., Logan, B.E., 2011. A method for high throughput bioelectrochemical research based on small scale microbial electrolysis cells. Biosens. Bioelectron. 26, 4526–4531.

Carrillo-Peña, D., Mateos, R., Morán, A., Escapa, A., 2022. Reduced graphene oxide improves the performance of a methanogenic biocathode. Fuel 321, 1–11.

Ceballos-Escalera, A., Molognoni, D., Bosch-Jimenez, P., Shahparasti, M., Bouchakour, S., Luna, A., Guisasola, A., Borràs, E., Della Pirriera, M., 2020. Bioelectrochemical systems for energy storage: a scaled-up power-to-gas approach. Appl. Energy 260, 1–12.

Cheng, S., Xing, D., Call, D.F., Logan, B.E., 2009. Direct Biological Conversion of electrical current into methane by Electromethanogenesis. Environ. Sci. Technol. 43, 3953–3958.

Chestney, N., 2022. Factbox: Europe takes action in case Russian gas supply stops. https://www.reuters.com/business/energy/european-measures-case-russian-gas-supply-stops-2022-06-21/. (Accessed 28 June 2022).

Deutzmann, J.S., Sahin, M., Spormann, A.M., 2015. Extracellular enzymes facilitate electron uptake in biocorrosion and bioelectrosynthesis. American Society for Microbiology 6.

Deutzmann, J.S., Kracke, F., Spormann, A.M., 2023. Microbial electromethanogenesis powered by curtailed renewable electricity. Cell Reports Physical Science 4, 101515.

Dunsing, V., Irmscher, T., Barbirz, S., Chiantia, S., 2019. Purely Polysaccharide-based Biofilm Matrix Provides Size-Selective Diffusion Barriers for Nanoparticles and Bacteriophages. Biomacromolecules 20, 3842–3854.

Enzmann, F., Holtmann, D., 2019. Rational Scale-up of a methane producing bioelectrochemical reactor to 50 L pilot scale. Chemical Engineering Science 207, 1148–1158.

Fasihi, M., Efimova, O., Breyer, C., 2019. Techno-economic assessment of CO2 direct air capture plants. J. Clean. Prod. 224, 957–980.

Fu, Q., He, Y., Li, Z., Li, J., Zhang, L., Zhu, X., Liao, Q., 2022. Direct CO2 delivery with hollow stainless steel/graphene foam electrode for enhanced methane production in microbial electrosynthesis. Energ. Conver. Manage. 268, 1–9.

Geppert, F., Liu, D., van Eerten-Jansen, M., Weidner, E., Buisman, C., Ter Heijne, A., 2016. Bioelectrochemical Power-to-Gas: State of the Art and Future Perspectives. Trends Biotechnol. 34, 879–894.

Hallam, S.J., Putnam, N., Preston, C.M., Detter, J.C., Rokhsar, D., Richardson, P.M., DeLong, E.F., 2004. Reverse methanogenesis: testing the hypothesis with environmental genomics. Science (New York, N.Y.) 305, 1457–1462.

Jiang, B., Yu, L., Wu, L., Di, Mu, Liu, Le, Xi, J., Qiu, X., 2016. Insights into the Impact of the Nafion Membrane Pretreatment Process on Vanadium Flow Battery Performance. ACS Appl. Mater. Interfaces 8, 12228–12238.

Kim, Y.S., 2014. Development and application of rapid methods for quantification and cultivation of methanogens in biomethane producing fermentors. PhD Thesis at University of the West of Scotland, 170 pp.

Kuwertz, R., Kirstein, C., Turek, T., Kunz, U., 2016. Influence of acid pretreatment on ionic conductivity of Nafion® membranes. J. Membr. Sci. 500, 225–235.

Lienemann, M., Deutzmann, J.S., Milton, R.D., Sahin, M., Spormann, A.M., 2018. Mediator-free enzymatic electrosynthesis of formate by the Methanococcus maripaludis heterodisulfide reductase supercomplex. Bioresour. Technol. 254, 278–283.

Lohner, S.T., Deutzmann, J.S., Logan, B.E., Leigh, J., Spormann, A.M., 2014. Hydrogenase-independent uptake and metabolism of electrons by the archaeon Methanococcus maripaludis. ISME J. 8, 1673–1681.

Maus, I., Kim, Y.S., Wibberg, D., Stolze, Y., Off, S., Antonczyk, S., Pühler, A., Scherer, P., Schlüter, A., 2017. Biphasic Study to Characterize Agricultural Biogas Plants by High-Throughput 16S rRNA Gene Amplicon Sequencing and Microscopic Analysis. J. Microbiol. Biotechnol. 27, 321–334.

Mayer, F., Enzmann, F., Lopez, A.M., Holtmann, D., 2019. Performance of different methanogenic species for the microbial electrosynthesis of methane from carbon dioxide. Bioresour. Technol. 289, 1–10.

Mayer, F., Sabel-Becker, B., Holtmann, D., 2022. Enhanced Electron Uptake and methane production by Corrosive Methanogens during Electromethanogenesis. Microorganisms 10, 2237.

Mohan, S.V., Sravan, J.S., Butti, S.K., Krishna, K.V., Modestra, J.A., Velvizhi, G., Kumar, A.N., Varjani, S., Pandey, A., 2019. Microbial Electrochemical Technology: Emerging and Sustainable Platform. Microbial Electrochemical Technology, 16 pp.

Nettmann, E., Bergmann, I., Mundt, K., Linke, B., Klocke, M., 2008. Archaea diversity within a commercial biogas plant utilizing herbal biomass determined by 16S rDNA and mcrA analysis. J. Appl. Microbiol. 105, 1835–1850.

Park, D.H., Laivenieks, M., Guettler, M.V., Jain, M.K., Zeikus, J.G., 1999. Microbial utilization of Electrically Reduced Neutral Red as the Sole Electron Donor for growth and Metabolite Production. Appl. Environ. Microbiol. 7, 2912–2917.

Pawar, A., Karthic, A., Lee, S., Pandit, S., Jung, S.P., 2021. Microbial electrolysis cells for electromethanogenesis: Materials, configurations and operations. Environmental Engineering Research 27, 200484–0.

Pelaz, G., González, R., Morán, A., Escapa, A., 2023. Elucidating the impact of power interruptions on microbial electromethanogenesis. Appl. Energy 331, 1–9.

Rabaey, K., Rozendal, R.A., 2010. Microbial electrosynthesis - revisiting the electrical route for microbial production. Nat. Rev. Microbiol. 8, 706–716.
Rowe, A.R., Xu, S., Gardel, E., Bose, A., Girguis, P., Amend, J.P., El-Naggar, M.Y., 2019. Methane-Linked Mechanisms of Electron Uptake from Cathodes by Methanosarcina barkeri. Applied and environmental Science 2, 1–12.
Scherer, P., 1989. Medium design for mass cultivation of methylotrophic methanogens: optima curves for gas evolution rates and growth yields of some new, precisely dosable inorganic and organic sulfur sources in comparison with H2S. Dechema Biotechnology Conferences 1- VCH Verlagsgesellschaft, 447–456.
Schorn, S., Ahmerkamp, S., Bullock, E., Weber, M., Lott, C., Liebeke, M., Lavik, G., Kuypers, M.M.M., Graf, J.S., Milucka, J., 2022. Diverse methylotrophic methanogenic archaea cause high methane emissions from seagrass meadows. Proceedings of the National Academy of Sciences of the United States of America 119.
Scott, K., Yu, E.H. (Eds.), 2015. Microbial Electrochemical and Fuel Cells: Fundamentals and Applications. Elsevier Science, Amsterdam, Boston, Cambridge, Heidelberg, London, 411 pp.
Siegert, M., Yates, M.D., Spormann, A.M., Logan, B.E., 2015. Methanobacterium Dominates Biocathodic Archaeal Communities in Methanogenic Microbial Electrolysis Cells. ACS Sustain. Chem. Eng. 3, 1668–1676.
Song, T.-S., Wang, G., Wang, H., Huang, Q., Xie, J., 2019. Experimental evaluation of the influential factors of acetate production driven by a DC power system via CO2 reduction through microbial electrosynthesis. Bioresour. Bioprocess. 6.
Völler, D., Wirth, V., Ehret, R., 2020. Evaluation of Bioelectromethanogenesis Part. Environmental Impact. Chemie Ingenieur Technik, II. https://doi.org/10.1002/cite.201900182.
Wolin, E.A., Wolfe, R.S., Wolin, M.J., 1964. Viologen dye inhibition of methane formation by Methanobacillus omelianskii. J. Bacteriol. 87, 993–998.
Xavier, K.V.M., Souza, E.S.e., Santos, E.d.A., Diniz, M.C., 2020. Genetic diversity of 16S rRNA and mcrA genes from methanogenic archaeas. Acta Sci. Biol. Sci. 42, e49877.
Yates, M.D., Siegert, M., Logan, B.E., 2014. Hydrogen evolution catalyzed by viable and non-viable cells on biocathodes. Int. J. Hydrogen Energy 39, 16841–16851.
Zakaria, B.S., Barua, S., Sharaf, A., Liu, Y., Dhar, B.R., 2018. Impact of antimicrobial silver nanoparticles on anode respiring bacteria in a microbial electrolysis cell. Chemosphere 213, 259–267.
Zhang, X., Bauer, C., Mutel, C.L., Volkart, K., 2017. Life Cycle Assessment of Power-to-Gas: Approaches, system variations and their environmental implications. Appl. Energy 190, 326–338.